LoRa Based Metrics Evaluation for Real-Time Landslide Monitoring on IoT Platform

SWAPNIL BAGWARI [1], **AJAY ROY**[1], **ANITA GEHLOT** [2], **RAJESH SINGH** [2],
NEERAJ PRIYADARSHI [3], (Senior Member, IEEE),
AND BASEEM KHAN [4], (Senior Member, IEEE)

[1]School of Electronics and Electrical Engineering, Lovely Professional University, Phagwara, Punjab 144411, India
[2]Division of Research & Innovation, Uttaranchal University, Dehradun, Uttarakhand 248007, India
[3]CTiF Global Capsule, Department of Business Development and Technology, Aarhus University, 7400 Herning, Denmark
[4]Department of Electrical and Computer Engineering, Hawassa University, Hawassa 05, Ethiopia

Corresponding author: Baseem Khan (baseem.khan04@gmail.com)

ABSTRACT In the context of an early warning system for landslides, monitoring of prone areas is a long-lasting process, little human intervention, and a resource less environment. Data changes in the monitoring area may be noticed in many days, months, or years depending on the weather characteristics. Therefore, a frequent and large amount of data of monitored area is not required to send on a cloud server. Moreover, Long-range communication provided comprehensive spectrum communication protocol and low power consumption with fewer data rates. Over the advantage of LoRa technology, we designed a customized sensor node and gateway node to monitor the changes periodically with low energy power consumption. We evaluated the distinct metrics of spreading factor, sensitivity, time-on-air, energy consumption, link budget, and battery life of sensor and gateway nodes. Finally, this study concludes with challenges faced in real-time in which the sensor data received via a customized sensor node and gateway on the cloud server.

INDEX TERMS Landslide monitoring, customized node, the IoT, long range radio, LoRa link budget, Fresnel zone, LoRa sensitivity.

I. INTRODUCTION

The threat of landslides rises every year because of the more rainfall caused by climate change. Additionally, secondary causes such as wildfires play a significant part in boosting landslides [1]. The poorest residents tend to be the most at risk of landslides because they live in many dangerous areas in many instances. That is especially true in the Andes, where more than 10 million people have been exposed to natural hazards, and a high amount of inequality is prevalent [2]. Back in Colombia, recent developments have contributed to a heightened rural depopulation and migration to cities. The result has been an unprecedented increase in the number of landslide casualties over the last 50 years, affecting more than half a million families from the past 100 years [3], [4]. Rainfall is the most critical triggering mechanism for all these landslides, though human hindrance is also an important cause. However, the advancement in IoT technology and low power wide area networks remote sensing is (LPWAN)

The associate editor coordinating the review of this manuscript and approving it for publication was Young Jin Chun [ ].

networks on research and professionals have also been observed. The industry seems to be more centered on pushing LoRa-based technologies to support human society [5]. LoRa-based IoT environment offers multidimensional implementation across diverse realms. LoRa architecture contains a sensor node known as end devices, a gateway that connects end devices with servers. The server stores all locally modified details on the cloud later level. By 2020, more than 25 billion devices have been expected to be wirelessly linked and to communicate with each other. In this context, the influence of such a technology might be visualized that could drive society to different degrees of demand [6], [7]. A prominent communication protocol on the IoT platform is LoRa (long-range). LoRa originates from a modulation technique called Chirp Spread Spectrum. LoRaWAN is exceptionally energy-efficient, consumes relatively low energy, and extends across a broad spectrum of wireless communication. Generally, battery-operated between the LoRa alliances and is connected to significant effects with a distance of between 2 to 3 km. It offers links and bridges networking protocols among BLE, GPRS, and Wi-Fi [5]. LoRaWAN is capable of

providing better efficiency between transmitter and receiver. Servers and gateways are linked through IP connection in a star topology. By hop link arrangement can be established many to many, many to one or one to many. Information is transmitted and received by all nodes within the network. LoRa is best suited for remote applications in which end nodes are deployed remotely at a long distance. IoT devices are becoming more popular and widely used than Wi-Fi that runs at 2.4 GHz because of their advanced features. However, LoRa does have some limitations on data transfer rates. LoRa's bitrate is below the Wi-Fi, which is between 20 and 30 Kbps. The main contributions of study are follows:

- The landslide monitoring system is integrated with low cost, low power and long-range communication. The Autonomous architecture is designed and implemented to optimize resources.
- LoRa SX1278 integrated with Wi-Fi ESP8266 architecture established the connection between the sensing unit and the IoT server.
- We have extensively different metrics such as link budget, time on-air, data rates, and battery life in different frequency ratios (7.8KHz, 20.8KHz, 31.25KHz, 41.7KHz, 62.5KHz, 125KHz, 250KHz, 500KHz) and spreading factor from 12 to 7.
- A customized sensor node, coordinator module and gateway module, battery consumption percentage is presented in different stages such as active, measurement and transmission stage.
- Fresnel zone study presented for real-time deployment scenario for low signal loss.
- The experimental study indicates the feasible layout of end nodes and gateways to bridge connectivity over the IoT network.

II. RELATED WORK

The LPWAN draws a lot of interest because of its shallow power usage. This system has the capability to communicate data over an extensive range of kilometres, with no wires, and can even communicate with hundreds of IoT devices without interference by people [6], [7]. This methodology simplifies applications like smart city, intelligent waste treatment, light automation, parking management, and intelligent agriculture [8], [9]. LoRaWAN technology is primarily a battery-operated convention used to connect and monitor appliances with several sensors and actuators [7]. New technologies comprise technological advances LoRa and NBIoT are securers compared to other protocols due to their improved capabilities [10]. This article [11] addresses the impact of fifty relevant articles where the application context, LoRa categorization, and at last, some conclusions to use this infrastructure are provided to have the strategy to create LoRa-based IoT framework solutions. A LoRaWAN-based architecture was developed for underground computerization. Challenges were found, like blind-spot identification, where no signal occurs, and a solution was provided to eliminate these communication problems [12]. Based on transmission spectrum

data from the life span of LoRa devices, the transmission of information of 100 bytes in a single day can be enhanced to 17 years [13]. The IoT's worldview is planning for an environment where a substantial part of our everyday items interconnect and interact with their state to gather information and computerize those activities [14]. A cloud-enabled framework was introduced incorporating different cloud technologies to promote user-friendly applications. Analytical instruments were available engaged in the collection of acceptable communication protocol over IoT platforms to analyze various parameters [15], [16]. At the same time, already extensive cloud computing and fog computation have suitable tools and solutions for keeping, collecting, and sharing the considerable quantity of IoT device data [17]. A comparative comparison of IoT and cloud architectures, comprising quality of service and availability, is presented in this article [18]–[20]. A complete assessment of various IoT technologies is mentioned in this article. The application design for the best techniques, such as LoRa, NBIoT, and Sigfox, is also outlined. The study addresses concerns about the criteria such as distance performance, power consumption, scalability, and cost [21]. For early warning systems for landslide monitoring, the recommended two-tier IOT network includes WSN and GPRS. The system consists of an unreliable multi-node system to detect appropriate changes from the area at risk of sliding and to communicate moisture, tilt angle and temperature data via the WSN S X1212 module at low power. The method also considerably enhances landslide surveillance prevention, efficiency and management [22]. The authors [23] used IoT technology in the field of landslides using customized sensor devices with independent sensing modules. The modules collect sensory data regularly using a low cycle and fetch data from the ELK stack utilizing the Sigfox network to the server. The devices improve the outcome of monitoring techniques such as installation, scaling, costs, accuracy, and remote raw data gathering in long-rang and close to real-time. Moreover, data mining shows significant result for landslide database creation and provides proper risk mitigation planning [24]. Table 1 shows different low power wide area network technologies available and compared in different metrics.

III. ARCHITECTURE OF LoRaWAN

LoRaWAN customized architecture is used to establish data links among the network and application layer. The architecture of LoRa constitutes an end node device, gateway, network server, and application layer. End nodes consist of sensor arrays and radio modules that are deployed on the ground. End nodes could be modified according to the specific requirement. In the proposed system, accelerometers, soil moisture, rainfall sensor, humidity and temperature sensor, and rain gauge are connected with the controller and further transmit the field's data. The end nodes share information with the server through a gateway. The intermediate network provided communications between the end nodes and the servers. The gateway module supports two different radio

S. Bagwari *et al.*: LoRa Based Metrics Evaluation for Real-Time Landslide Monitoring on IoT Platform

TABLE 1. Different LPWAN's technologies comparative analysis [25].

Technology	Range in KM (Urban, Rural)	Packet Size	Modulation	Downlink Communication	Duplexing	Operating Frequencies	Encryption	Sleep mode	Transmission (), Tx, Rx Power()	Battery Life
LoRaWAN	5,18	19-250 Bytes	LoRa C-SS	Yes	HD C-SS	433/868/780/915 MHz ISM	AES-128	1μA	14-27 dBm 28 10.5	10Years (3.6V lithium AA-cell)
SigFox	10, 50	12 Bytes UL, 8 Bytes DL	DBFSK(Uplink) GFSK(Downlink)	Very Limited	Limited HD	Between 865-924 MHz	Optional AES-128	6nA	14-12 dBm 10-50 mA 10 mA	10 Years (9V Battery)
LTE-M	<11, 11	up <1 Mbps, down < 1 Mbps	BPSK,QPSK,16QAM,64QAM	Yes	FD,HD FDD,TDD	LTE Licensed	3GPP 128-256 bit	8 μA	20dBm 300mA 53.33mA	10 Year (5Wh Battery)
NB-IoT	<100,100	200 kbps	QPSK	Yes	HD FDD	LTE Licensed	3GPP 128-256 bit	3 μA	20-23 dBm 74-220mA 46mA	10 Year (5Wh Battery)
Wightless-P	2 to 5, 25	5-260 Bytes (GMSK) 131-514 Bytes (OQPSK)	GMSK, offset-QPSK	Yes	HD	Sub -GHz ISM	AES-128 AES - 256	<4 μA	15 dBm 49mA 13mA	3-8 (Coin Cell)
NB-Fi	10, 30	Unknown	DBPSK	Yes	Full Duplex	433/868.8/915 MHz ISM	XTEA-256	1.5 μA	14-27dBm 44mA 12mA	20 Years (AA-cell)
DASH7	2 KM	0-256 Bytes	2-GFSK	Yes	Half Duplex	433/868/915 MHz ISM	AES-128	1-2 μA	10 dBm 29.2mA 15mA	10 Years (Coin Cell or thin-film)
EC-GSM	<15,15	Unknown	GMSK, 8PSK	Yes	HD FDD	GSM Licensed	3GPP 128-256 bit	10 μA	23 or 33 dBm 123,1228 mA 66 mA	10-14 years (5Wh battery)

frequencies to connect nodes with each other. Every device will be connected through a unique identification number to the gateway. The network server records all validating data generated by sensors. It is designed to evaluate quantitative data and decide what the appropriate data is using these analytics. The network server connects to the gateway module by using an Ethernet cable or through a wireless connection. These are the last phases of this framework in which all sensor node activity is controlled via an application interface. The platform offers many features, including file transfer, email, and web services. It could be any interaction with a device, such as a GUI or a mobile app. This layer works primarily with the client. It requires effective communication with both the process and communication between machines to machine.

A. LoRa OVERVIEW

LoRa is a standardized physical layer (PHY) specification developed by Semtech for long-range, low-power networks [26]. This technology allows for connecting intelligent devices with a distance of kilometres importantly, with low power consumption. The LoRa system has been developed to support the LPWAN, which operates the 433 MHz (Asia), 915 MHz (North America), and 868 Mhz (Europe) which utilize ISM bands (Industrial, Scientific, Medical) [7]. To accomplish this, LoRa develops a spectral spreading modulation technique, a type of CSS (Chirp Spread Spectrum) [27], to modulate frequency without changing the phase of symbols [28] and data encoding [26], [29]. The top layer is in the LoRaWAN protocol stack is the application layer. The physical layer is responsible for modulation under the regional ISM band. Data link layer designed by LoRa alliance. This layer use ALOHA medium access control mechanism [30] with the association of three end devices classes, i.e. Class A, B, and C. The physical layer used CSS transmission with configurable parameters such as Bandwidth, Spreading Factor, Carrier Frequency, Transmission power, and coding rate. SF is the primary quality of service assurance parameter. The transmission rates are much higher and air time low whenever the smaller range of SF values is

being used. The greater the number of SFs, extend the range. However, it limits the Quality of Service (QoS). SFs from 7 to 12 permit transverse communication, ensuring that various networks can communicate in the same frequency spectrum at the same time without interfering. Equation (1) specifies the transmission rate, and the bandwidth ratio between SF (Spreading Factor), Bandwidth (BW), and Symbol Rate (RS)
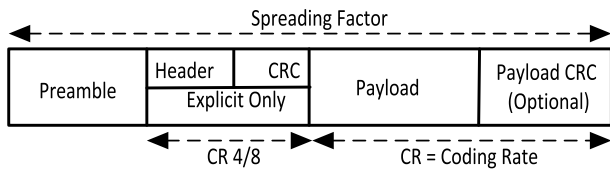
$$RS = \frac{BW}{2^{SF}} \qquad (1)$$

FIGURE 1. LoRa packet structure.

LoRa frame format can sometimes be implicit or explicit where explicit packets include header contains byte information, CRC, and frame code rate information. LoRa packet structure shown in Figure 1 comprises three elements, i.e., a preamble, an optional header, and the data payload. The preamble synchronizes the receiver with the inward flow of information. The packet is set to a 12-symbol sequence by default. Because of the potentially long packet duration with significant spreading factors, it is possible to increase the transmission stability to changes in frequency over the transmission and the reception periods of the packet [31]. Time on Air is a critical parameter issue for real-time applications. Transmit LoRa frame can be calculated by knowing the values of CR, BW, and SF, which is the summation of preamble time and the payload as defined in Equation (2).

$$T_{frame} = T_{preamble} + T_{payload} \qquad (2)$$

$T_{preamble}$ is depend on the T_{sym} and programmable length of the preamble $n_{preamble}$. In the case of our study, we used a preamble value of 8 as fixed in the case of LoRaWAN 1.0 [28].

$$T_{sym} = \frac{1}{RS} \qquad (3)$$

With Equation (1) we will define the symbol duration, T_{sym} by the following equation (4)

$$T_{sym} = \frac{2^{SF}}{BW} \qquad (4)$$

$$T_{preamble} = (n_{preamble} + 4.25)\, T_{sym} \qquad (5)$$

The payload is depends also on the option enabled, and this equation determines the quantity of the payload symbol.

$$n_{payload} = 8 + \max$$
$$\times (\text{ciel}\left[\frac{(8PL - 4SF + 28 + 16RC - 20IH)}{4\,(SF - 2DE)}\right]$$
$$\times\,(CR + 4)\,, 0) \qquad (6)$$

where PL indicates the number of payloads bytes range from 1 to 255, SF shows the spreading factor from {6,7,8,9,10,11,12}, if DE = 1 when LowDataRateOptimize = 1, otherwise DE is 0, CR is the coding rate from 1 to 4, IH = 0 means header is enabled otherwise no header is available in the case of 0 [32]. The payload duration is known by the symbol period multiplied by the number of payloads as shown in Equation (7).

$$T_{payload} = n_{payload} \times T_{sym} \qquad (7)$$

Bit Rate is the rate of transmission of bits from one region to another. LoRa Bit Rate (R_{bit}) is indicated as

$$R_b = SF \times \frac{\left[\frac{4}{4+CR}\right]}{\left[\frac{2^{SF}}{BW}\right]} \qquad (8)$$

Sensitivity is the quality associated with the ability of a system to retrieve features from signals. The signal strength can also be measured as low as possible, prompting the device to its packet interpretation. The receiver sensitivity of LoRa at room temperature in equation (9) where (-174) is taken because of the receiver's thermal noise at a bandwidth of 1Hz, NF represents the Noise Figure of the receiver, and SNR represents modulations signal-to-noise ratio.

$$S = -174 + 10log_{10}Bw + NF + SNR \qquad (9)$$

For the optimal decisions, the length of the spread depends on the ratio of "chips per bit." The chip sequence ratio to the desired data speed is often described as the Gp (processing gain) and expressed in dB.

$$G_p = 10 \times log_{10}\left(\frac{R_c}{R_b}\right) \qquad (10)$$

where R_c is chip rate (chips/second) and R_b is bit rate (bit/second). The process gain of the receiver will considerably reduce interfering signals. These can be deleted using filtering over the appropriate information bandwidth.

B. LoRaWAN TRANSACTIONS

The protocol stack standard, LoRaWAN, defines three device classes with two-way communication in accordance with downlink latency and power limitations. Due to higher latency, Class A devices have longer battery life. After an Uplink broadcast, the downlink happens in two windows and is delayed [33].

AT SF 7, it takes 5.1ms and a maximum of 164ms at SF12 data rates. Moreover, it takes less than 100ms to demodulate the signal and more than 2 seconds in SF12 typically while sleep periods of the end device are 1ms with 1μA current rating [31]. The length of each window should be as much as the time required to detect the downlink preamble by the endpoint radio transceiver successfully. If the device detects a downlink preamble at this period, the radio receiver remains open until the downlinks are demodulated. The LoRaWAN Class A operation is shown in Figure 2.
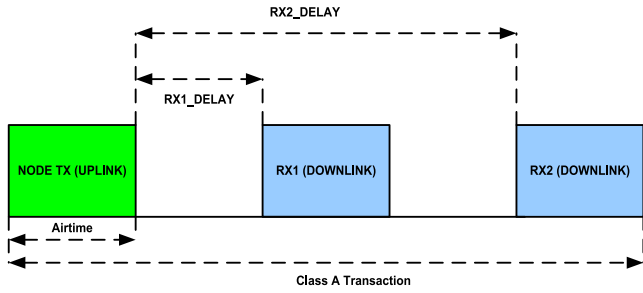
FIGURE 2. LoRaWAN Class A Scheme.

Downlinks from a base station to the previously set periods are scheduled by Class B devices to determine if applications can deliver control messages to end devices [34]. For class A, the downlink windows for Class B transactions occur at particular periods following a beacon, as shown in figure 3. On the other hand, class C devices are powered by the grid and always listen to the media and receive low latency downlink transmissions. Therefore, it contains windows that remain practically always open (locked except during transmission), as shown in Figure 4.
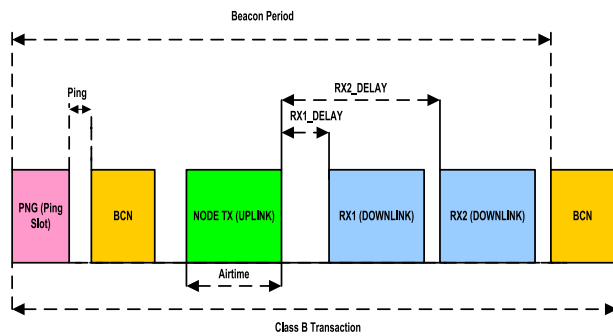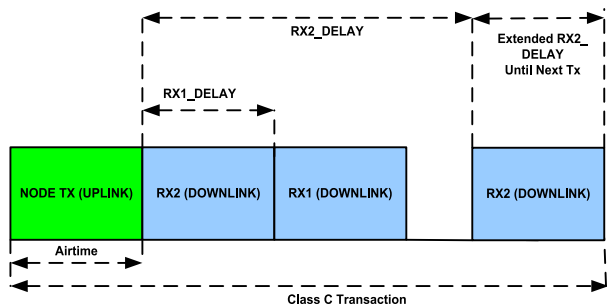

FIGURE 3. LoRaWAN Class B Scheme.

FIGURE 4. LoRaWAN Class C Scheme.

IV. SYSTEM ARCHITECTURE AND DESIGN

Internet of Things (IoT) based landslide-prone area monitoring nodes are implemented to precisely monitor the changes of slope stability and respond it to timely in cloud services to perform further required steps. The sensor node, coordinator node, and gateway node designed to consume low power and cover a long communication range for the betterment of society. Nodes provide numerous data periodically from

the field and further analyze the data to promote effective decisions. The proposed architecture is shown in the Figure 5. End nodes consist of sensors and Zigbee to cover a part of the landslide area. Sensors used in this proposed system are 3-axis Accelerometer, Soil moisture, Rainfall sensor, Rain gauge, and sound sensor. Multiple nodes are placed in a different area, and using Zigbee personal area network is created. Zigbee end node transmitted data to nearest Zigbee coordinator, and further data is transferred to long-range using LoRa module. A LoRa-enabled architecture for slop monitoring was exhibited in which LoRa allowed every node to connect with another LoRa-enabled sensor and establish a communication channel. LoRa is a technology that offers minimal power and an extensive range of communication to transmit and receive. While there are many alternative protocols, all have significant limits on LoRa. In this study, we have an extensive analysis of the LoRa communication link but not for the personal area network created by Zigbee. A gateway is placed to received data from long-range radios and further transmitted to the cloud using a Wi-Fi modem. Cloud analytics proposed the intimation to customers from any upcoming disaster.
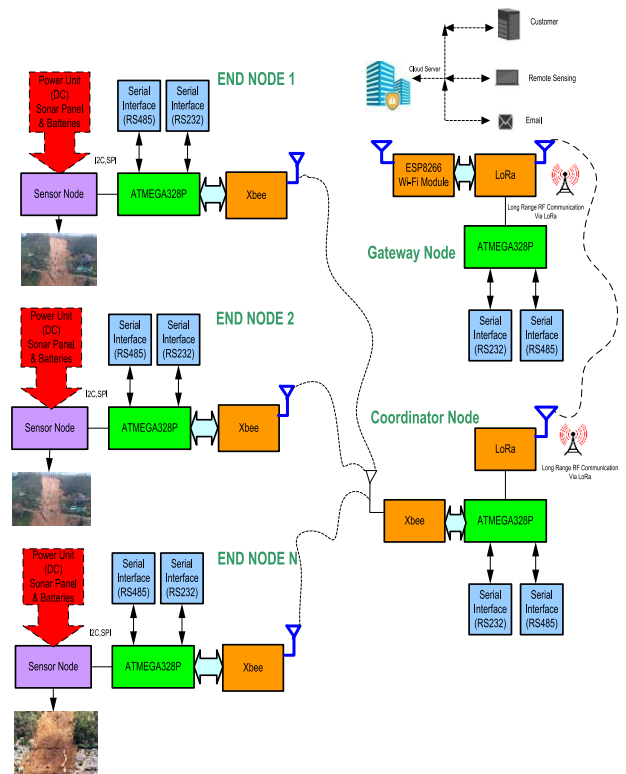

FIGURE 5. IoT based block diagram for landslide monitoring.

The hardware setup is outlined in this section. Section 3.1 details the fabrication of the system. PCB trace software was used to achieve the custom design after that assembling of components performed. The customized LoRa system is shown in Figures 6, 7, and 8 as sensor node,

coordinator node, and gateway node, respectively. This device contains an ATMEGA328p microcontroller, a power source, a LoRa modem, a sensor array that integrates with various external sensors. ATMEGA328 is an 8-bit high-end reduced instruction set computer-based microcontroller with 32 KB of read-and-write ISP flash memory and 23 GPIO pins, and 10-bit ADC. It has 14 digital pins and six analog pins. It supports a master/slave SPI serial interface and easy to perform in-system programming using Arduino IDE. In the active state, it consumes 1.5mA at 3V, and in power-down is the only $1\mu A$ at 3V. Therefore, it operates a voltage between 1.8 and 5 V. The voltage then passes through the voltage regulator ICs (IC7805 and IC7812). The IC7812 is a low-cost regulator IC which yields 12V output voltage. The terminals are three pins IN, COM and OUT. To track the operational status of the power supply unit, an LED indicator has been attached. Similarly, IC7805 is a regulator linked to a source of 5 V. These two ICs belong to the same family of 78xx ICs.

The SX1278 LoRa transceiver used in this study works in an ISM band frequency of 433MHz. All the experimentation done in further sections is performed using the same frequency level. It supports network topology such as point to point, points to multipoint, peer to peer, and mesh. The data rate of SX1278 is less than 300kps. It supports modulation FSK/MSK/GFSK/LoRa with the operation voltage of 1.8V to 3.6V. The sensitivity of the LoRa module is -136dBm with an output power of $+20$ dB. SX1278 module consumes a current 120mA while transmitting and 10.8mA while receiving data packets. RSSI and Link budget of SX1278 LoRa module is 127dB and 168dB, respectively. The proposed customized board comprises 5V and 12V power supply variants. ATMEGA 328 Controller was used for the development and customization of this transmitter on a PCB. Digital, Analog, I2C, and SPI pins are available for sensor interfacing. Figure 6 demonstrates the custom configuration of the LoRa node system and contains several components. The controller is also attached to the SX1278 LoRa package, and the sensor data forwarded to the nearby available gateway. It includes a wide variety of pins to allow different sensors able to communicate with it. The LoRa architecture is regarded as an end unit. It has functioned on a rechargeable battery which can be used for stability monitoring in the landslide-sensitive region. The LoRa module has been implemented using an ATMEGA328p, including customized GPIO pins. DHT11 sensor monitored surrounding changes in temperature and humidity. DHT11 OUT PIN pin connected to digital pin 2 to ATMEGA328. Rainfall sensor, rain gauge sensor and soil moisture sensor connected to Analog pins of controller named A1, A2, and A3, respectively. Appropriate packaging is maintained in harsh environments to preserve the device.

The LoRa coordinator node block diagram is shown in Figure 7. All the transmitter module information is expected to be received by the LoRa receiver. It consists of Sx1278 LoRa Module, ATMEGA328p microcontroller, liquid crystal display and sensor array. The SX1278 is a LoRa
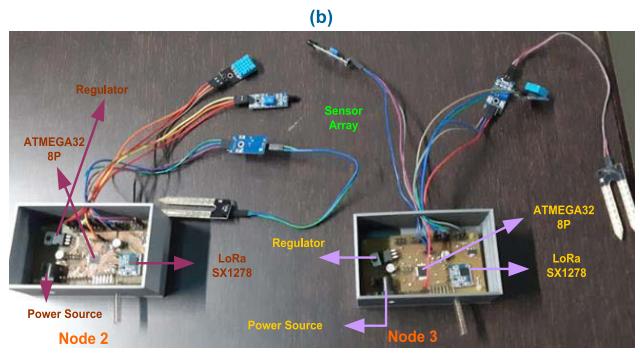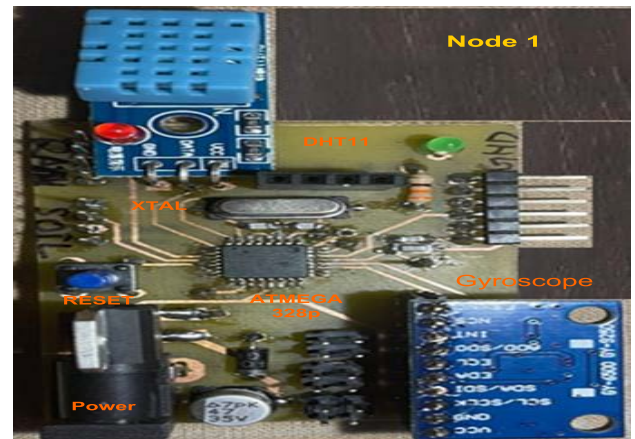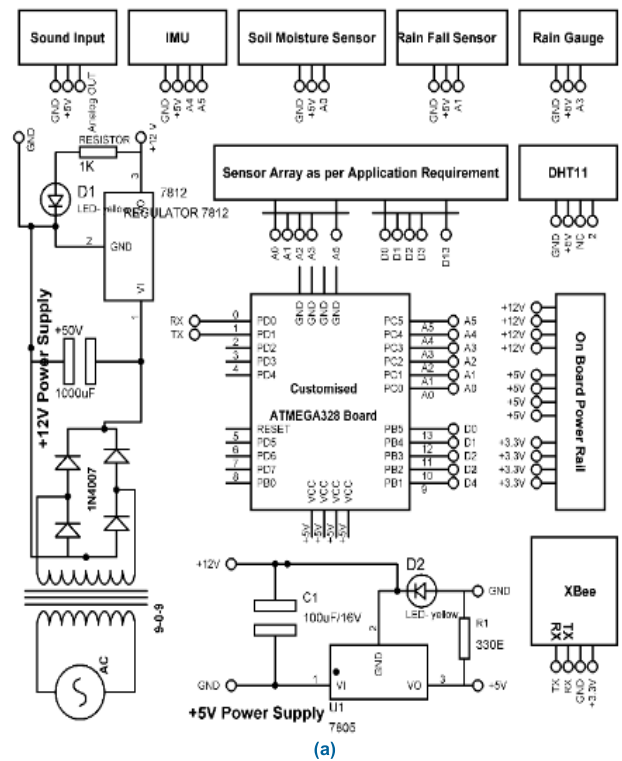

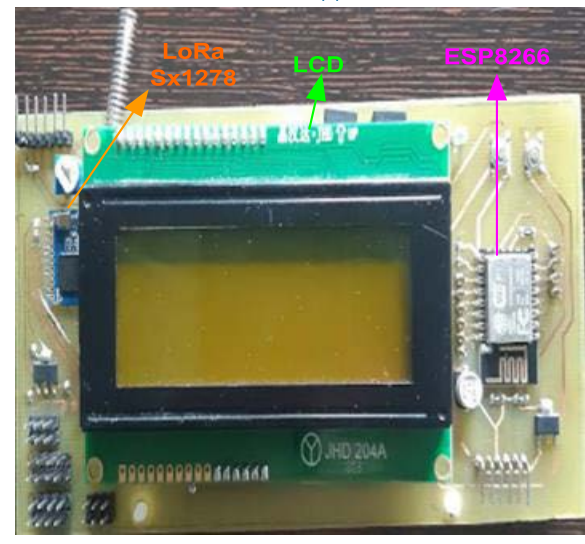**FIGURE 6.** (a) Symmetric diagram of end node (b) Customized node 1 (c) Customized sensor nodes 2 and 3.

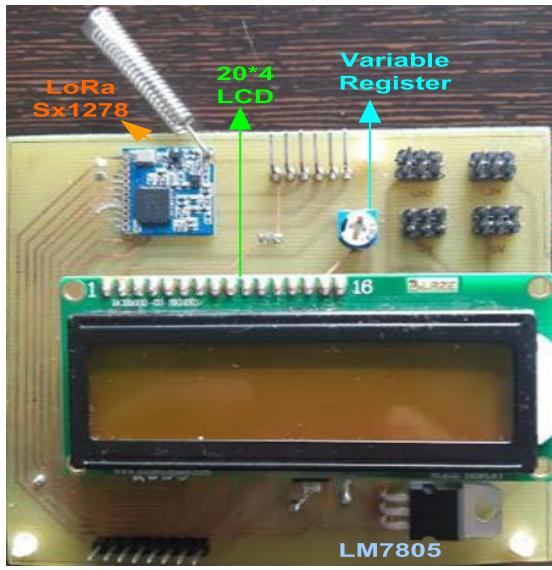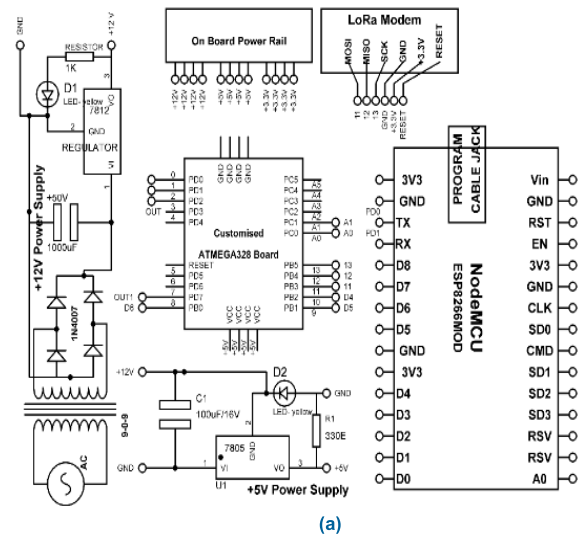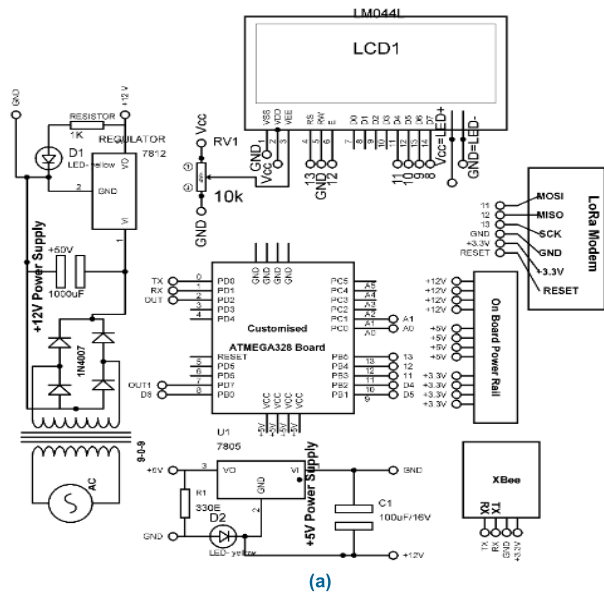FIGURE 7. (a) Symmetric diagram of coordinator node (b) Customized coordinator node.

FIGURE 8. (a) Symmetric diagram of gateway node (b) Customized gateway node.

transceiver developed by SEMTECH with various frequencies from 135 to 520 MHz with low power consumption. The advantages of the LoRa transceiver have listed in the form of a 168 dB connection budget, +20 dBm–100 mW steady RF output against V supply, +14 dBm high-efficiency PA and transmission bit rate 300 kbps [7], [8]. The variable register is also connected with LCD to fix the contrast according to the real-time visibility. Data can be transferred regionally and remotely through the receiver module. Figure 8 shows the block diagram of the gateway. Gateway has an additional module ESP8266 Wi-Fi module with LoRa Sx1278. Gateway is supposed to understand two different radio signals and works as a mediator between transmitter and receiver. It received data from the sensor array and sends

the information to the cloud server. The customized board is capable of working in +12V and +5V. Coordinator and gateway node consist of 20∗4 Liquid Crystal Display to show real-time data on the screen. LCD programmed using busy flag mode, i.e. monitoring of D7 bit to write data correctly, excluding the chances of missing data if programmed through delay method. It is interfaced using 4-bit mode with microcontroller ATMEGA328. Moreover, it saves four pins of the microcontroller. However, the potentiometer is connected with pin no.3 of LCD to control the contrast of LCD according to requirement.

ATMEGA328p microcontroller is capable of SPI and I2C communication. For SPI communication, master out slave in pin, master in slave out pin, serial clock pin, and the ground.

In each SF, the data rate increases with respect to an increase in bandwidth, i.e. 125KHz, 250KHz, and 500KHz has been interfaced with the LoRa modem. The sensor used in the application are required analog and digital pins of

the microcontroller to interface with sensors such as soil moisture, rainfall sensor, accelerometers, and rain gauge. The purpose of the software configuration is to provide a stable and reliable response from hardware devices. The software used to set up the LoRa test platform illustrates using a modeling tool and verifying the LoRa test platform until it has been fabricated. The designed layout was built on the Proteus simulation platform. The customized board is also incorporated with the boot loader to behave integrated chips perfectly. Integrated Development Environment is used for further programming part.

V. LoRa SENSOR SCALABILITY ANALYSES AND PERFORMANCE EVALUATION

A. BIT RATE AND TIME ON AIR

The rate/bit rate is defined as the total amount of bits transmitted between the transmitter to the receiver. Equation (3) has been used to get the LoRa data rate. The input parameters, such as CR, SF, and BW, are incorporated in the calculation to determine the LoRa data rate. We have considered bandwidth 125KHz, 250KHz, and 250KHz, spreading factor from 6 to 12, and coding rate from 1 to 4. SF6 is not a part of LoRaWAN but only for Lora capability [33] tested in the current study. The Figure 9, 10 and 11 shows the bit rate and time on Air in frequency 125KHz, 250KHz, and 500KHz respectively. The data rate is bits per second indicated (bps) and time on-air in a millisecond.

It can be observed that the data rate in SF7 for bandwidth is 5468 bps at CR1, 4557 bps at CR2, 3906 bps at CR3, and 3417 bps at CR4. It exponentially increased in the data rate of SF7 for bandwidth 250KHz is 10937 bps at CR1, 9114 bps at CR2, 7812 bps at CR3, and 6835 bps at CR4. However, bandwidth set to 500KHz provides a higher bit rate in the case of SF7, i.e. 21875 bps at CR1, 18229 bps at CR2, 15625 bps at CR3, and 13671 at CR4. The increase in SF7 affects the data rate counter as the data rate steadily decreases from SF 7 to SF 12. In our study, the LoRa has reached 21875 bps, 10937 bps, 5468 bps in SF 7, while the data rate in SF 12 has been limited to 1171 bps, 585 bps, and 292 bps at 500KHz, 250KHz, and 125KHz respectively at CR1. An increase in SF will result in the transmission of a small amount of data, which means that SF 7 is the ideal SF for transmitting a large number of data.

B. LoRA SENSITIVITY

There is a SNR$_{limit}$ for each spreading factor, such that the receiver cannot demodulate the signal if this limit is achieved. LoRa sensitivity includes the input spreading factor, the bandwidth, and the noise figures, and provides the output sensitivity. SNR$_{limit}$ is different for distinct spreading factor i.e. -20 for SF12, -17.5 for SF11, -15 for SF10, -12.5

In our study we set specific parameters in this investigation to calculate ToA such as Frequency = 433MHz, preamble = 8 bytes, payload = 100 bytes, Tx Power = 17 (dBm) and coding rate = 1,2,3 and 4. The ToA calculation tool is taken
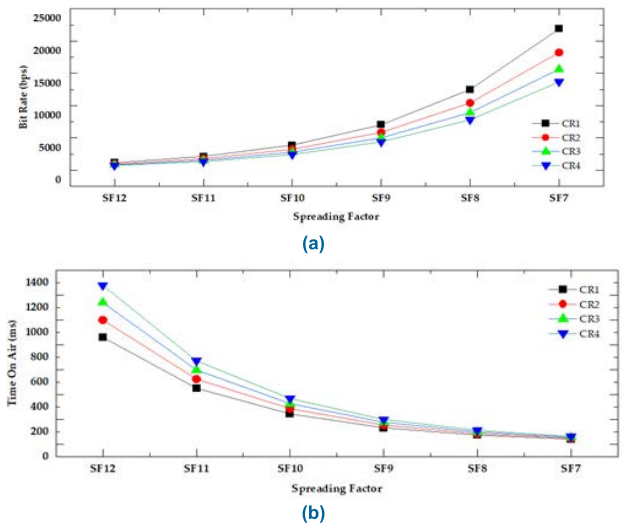
FIGURE 9. (a) Data rate at 500 KHz (b) ToA at 500 KHz.
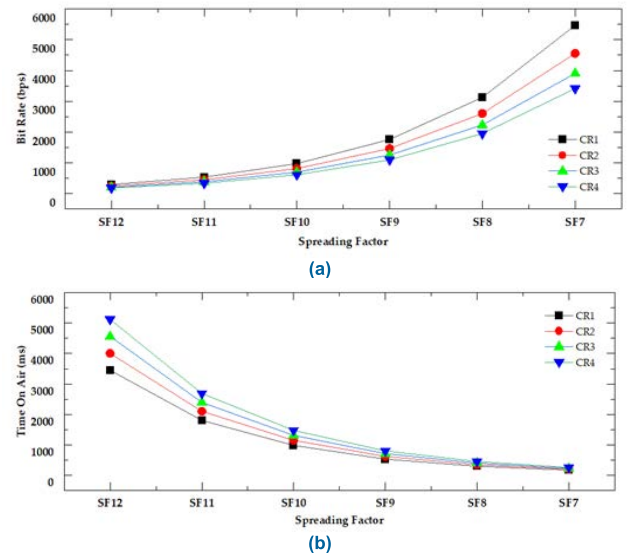
FIGURE 10. (a) Data rate at 125KHz (b) ToA at 125 KHz.

into consideration [32]. We set the same study indicators for data rates such as Bandwidth 125KHz, 250KHz, and 500KHz, Spreading factor from SF6 to SF 12, and Coding rate from 1 to 4. In the given tabular 2, 3 and 4 form, the measured results are presented. The graphs show a sudden increase in time on-air after spreading factor SF9 to SF12. The table 2, 3, and 4 represents ToA at 500KHz is 42.3ms, at 250KHz is 84.61ms and at 125KHz is 169.22 ms in the spreading factor of 7. This study shows that ToA is reduced by half when bandwidth rises from 125 kHz to 500 kHz. The figure 11 illustrates that the ToA increases whenever the SF shift from 7 to 12. for SF9, -10 for SF8 and -7.5 for SF7. As shown in Table 5 if the spreading factor increase by 1, changes of -2.5dB found in SNR$_{limit}$. To calculate receiver sensitivity, we utilized Equation 9. However, the NF (6 dB)

TABLE 2. Bit rate (bps), Time on air (ToA) (ms) at 500KHz.

SF	CR=1		CR=2		CR=3		CR=4	
	ToA	Bitrate	ToA	Bitrate	ToA	Bitrate	ToA	Bitrate
12	862.21	1171.88	1001.47	976.56	1140.74	837.05	1280	732.42
11	451.58	2148.44	525.31	1790.36	599.04	1534.6	672.77	1342.77
10	246.27	3906.25	287.23	3255.21	328.19	2790.18	369.15	2441.41
9	133.38	7031.25	155.9	5859.38	178.43	5022.32	200.96	4394.53
8	74.37	12500	87.17	10416.67	99.97	8928.57	112.77	7812.5
7	42.3	21875	49.73	18229.17	57.5	15625	64.58	13671.88

TABLE 3. Bit rate (bps), Time on air (ToA) (ms) at 250KHz.

| SF	CR=1		CR=2		CR=3		CR=4	
	ToA	Bitrate	ToA	Bitrate	ToA	Bitrate	ToA	Bitrate
12	1724.42	585.94	2002.94	488.28	2281.47	418.53	2560	366.21
11	903.17	1074.22	1050.62	895.18	1198.08	767.3	1345.54	671.39
10	492.54	1953.13	574.46	1627.6	656.38	1395.09	738.3	1220.7
9	266.75	3515.63	311.81	2929.69	356.86	2511.16	401.92	2197.27
8	148.74	6250	174.34	5208.33	199.94	4464.29	225.54	3906.25
7	84.61	10937.5	99.46	9114.58	114.3	7812.5	129.15	6835.94
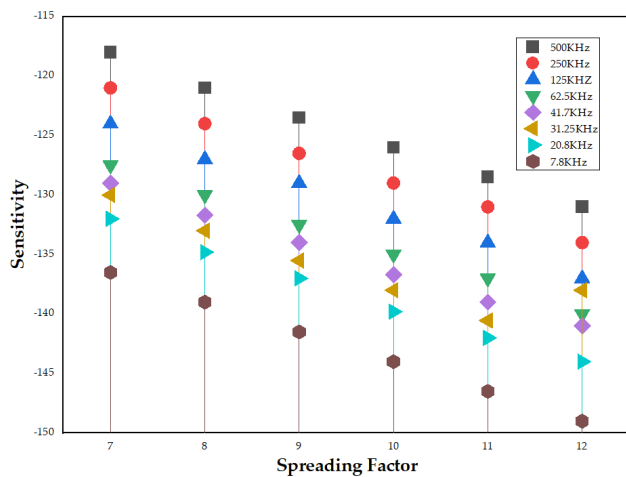
FIGURE 11. LoRa sensitivity (SF7-SF12).

is fixed for given hardware SX127 and depends on hardware implementation.

Depending on the network data rate and range required adjustments, if a change is made in the chosen spreading factor, sensitivity varies as well. As shown in Table 6 different frequencies have been used, and corresponding sensitivity is calculated according to the spreading factor. In general, the power sensitivity is a negative value, e.g. −127 dBm, if the value exceeds that number shows a decrease in the sensitivity. Figure 12 shows the sensitivity in different bandwidths with respect to the spreading factor. As we can observe, sensitivity

at 500KHz for SF 7 is highest, i.e. −118, and sensitivity at 7.8KHz for SF12 is lowest, i.e. −149.

For 5KM value is 0.59m, for 6KM value is 0.59m, for 7KM value is 0.80, for 9KM value is 1.33m and for 10KM value is 1.64m.

C. FRESNEL ZONE FACTOR

The Fresnel region is an elliptic shape spanning the direct line between the end node and the gateway. Any obstruction within this volume, such as buildings, plants, mountains, and the land, may weaken the broadcast signal, even though the end node and the gate are directly visible. The area should be free of obstacles of at minimum 60%, including buildings, mountain areas or trees [35]. This, like in our experiment, reduces the performance of wireless communication. Therefore, it is vital to have a clear sightline between the sender and receiver as far as possible. Results are calculated the maximum radius from the Fresnel zone half from the end node to the gateway.

$$r = 8.657\sqrt{\frac{D}{f}} \quad (11)$$

where r is Fresnel zone radius in meter (m), D is the distance in Kilometer (KM), and f is the frequency in GHz. The 20% obstruction in the Fresnel Zone typically entails minimal power losses towards the link signal loss. Over 40 percent obstruction is expected to be significant. It is recommended that a microwave path analysis be made for extended links, which considers it and the field topography. In our experiment, transmitter node and receiver, the node is fixed in

TABLE 4. Bit rate (bps), Time on air (ToA) (ms) at 125KHz.

	CR=1		CR=2		CR=3		CR=4	
SF	ToA	Bitrate	ToA	Bitrate	ToA	Bitrate	ToA	Bitrate
12	3448.83	292.97	4005.89	244.14	4562.94	209.26	5120	183.11
11	1806.34	537.11	2101.25	447.59	2396.16	383.65	2691.07	335.69
10	985.09	976.56	1148.93	813.8	1312.77	697.54	1476.61	610.35
9	533.5	1757.81	623.62	1464.84	713.73	1255.58	803.84	1098.63
8	297.47	3125	348.67	2604.17	399.87	2232.14	451.07	1953.13
7	169.22	5468.75	198.91	4557.29	228.61	3906.25	258.3	3417.97

TABLE 5. SNR_{limit} value for respective SF.

SF(Spreading Factor)	Chips/Symbol	SNR_{limit}
12	4096	-20
11	2048	-17.5
10	1024	-15
9	512	-12.5
8	256	-10
7	128	-7.5

31m and 50m, respectively. We considered an obstacle height in the range of 38m to 23m which makes an average of 30.5m. Fresnel Zone radius is calculated by equation (11) to calculate whether the obstacle creates degradation in signal performance. The Fresnel zone midpoint is 40.5, i.e., the transmitter height and receiver height further divided by two. Earth curvature value in m measured by the following formula.

$$H = \frac{1000 \times D^2}{8 \times R_{earth}} \quad (12)$$

where, H is Hight (or earth curvature allowance) in m, D is the distance between end node and gateway in KM and R_{earth} is earth radius in KM i.e. 8504KM.

The Fresnel Zone equation (11) is based on a flat earth and not considered the earth's curvature. This curvature also affect the data loss but found minor changes up to 5KM, i.e. for 1KM, the value is 0.014m, for 2KM the value is 0.058m, for 3KM value is 0.1322m, for 4KM value is 0.235m, for We found significant changes in the percentage of clear Fresnel zone with the consideration of earth curvature value from 5KM. Table 7 illustrates the results of Fresnel zone clearance decreases while increasing the distance. In addition, in which the percentage is greater than 60 percent, the link results are impacted [36]. Therefore, in this instance, this obstruction and the clear connectivity of the transmitter to the receiver node line-of-site are avoided.

D. LINK BUDGET

The power transmission balance or link budget has an important role to indicate the quality of the radio transmission channel. The relationship of link budget with sensitivity, transmit power (Tx), free space path loss, and gain is shown in Equation (9). We considered the same band-width as used in section 5.2 LoRa sensitivity i.e., 7.8KHz, 20.8KHz, 31.25KHz, 41.7KHz, 62.5KHz, 125KHz, 250KHz, and 500KHz with the spreading factor from 7 to 12. Link budget calculated and compared at different levels such as 4dBm, 7dBm, 11dBm, 14dBm, and 17dBm with frequency at 433MHz. As shown in figure 13, it is observed that an increase in the Tx found an increment in link budget with respect to bandwidth. For example in the case BW 7.8KHz for spreading factor 7 at 4dBm value is 140.5, at 7dBm value is 143.5, at 11dBm value is 147.5, at 14dBm value is 150.5 and at 17dbm value is 153.5. In contrast for spreading factor 12 at 4dBm value is 153, at 7dBm value is 156, at 11dBm value is 160, at 14dBm value is 163 and at 17dBm value is 166. It shows for every increment in SF, the link budget will also increase. At 17dBm, the link budget is maximum (151) for spreading factor 12 whereas the link budget is lowest (135) recorded at 4dBm for SF7. It is experienced that with maximum Tx power and low bandwidth achieved maximum link budget.

VI. BATTERY LIFE TIME

To achieve better utilization of battery power, systems should work efficiently in their states such as computation stage, communication stage, active stage, and sleep stage [35]. The measurement stage intends to provide power to all sensors for reading and writing the measurements values. This stage includes ADXL345 Accelerometer Sensor, DHT11 Temperature and Humidity Sensor, RG200 Rain gauge 6 Inch sensor, Rainfall sensor, FC-28 Soil moisture sensor. ADXL345 sensor is 3-axis digital accelerometer with 13-bit resolution and measurement from $\pm 2g$, $\pm 4g$, $\pm 8g$, to $\pm 16g$. It works in ultralow-power, i.e. $23\mu A$ in measurement mode and $0.1\mu A$ in standby mode at a voltage source of 2.5V. The sensor has 10,000g shock survival and a wide temperature range from -40°C to +85°C. Moreover, the ADXL345 sensor available in a small and thin plastic package of 3mm × 5mm × 1mm, suitable for this application. Our study found 60 times of reading in an hour consume only 0.005mA in a year and use the lowest percentage of battery, i.e. 0.5%. However, to monitor the changes on slop, many accelerometers are required, and by using table 8 we can compute the battery use. We found that the DHT11 sensor four-pin package used to monitor temperature and humidity has the highest

TABLE 6. LoRa sensitivity.

SF	500KHz	250KHz	125KHZ	62.5KHz	41.7KHz	31.25KHz	20.8KHz	7.8KHz
12	-131	-134	-137	-140	-141	-143	-144	-149
11	-128.5	-131	-134	-137	-139	-140.55	-142	-146.5
10	-126	-129	-132	-135	-136.7	-138	-139.8	-144
9	-123.5	-126.5	-129	-132.5	-134	-135.5	-137	-141.5
8	-121	-124	-127	-130	-131.7	-133	-134.8	-139
7	-118	-121	-124	-127.5	-129	-130	-132	-136.5

TABLE 7. Fresnel zone packet loss with frequency at 433MHZ.

Distance (m)	Radius (m)	Radius with curvature of earth surface (m)	Fresnel Zone Diameter (m)	Fresnel Zone Center Hight (m)	Obstacle Crossed Fresnel Zone (m)	Clear Fresnel Zone (m)
1000	13.51	13.52	27.02	28.99	1.51	94.40%
2000	18.60	18.65	37.20	28.4	7.10	80.90%
3000	22.78	22.91	45.56	19.72	10.78	76.33%
4000	26.31	26.54	56.62	16.19	14.32	74.70%
5000	29.41	29.77	58.82	13.09	17.41	70.40%
6000	32.22	32.81	64.44	10.28	20.22	68.60%
7000	34.80	35.6	69.60	7.70	22.80	67.20%
8000	37.21	38.15	74.42	5.29	25.21	66.12%
9000	39.46	40.79	78.92	3.04	27.46	65.20%
10000	41.60	43.24	83.20	0.90	29.60	64.42%

TABLE 8. Battery life calculation in active, measurement and transmission stage (available battery 8400MH.

			Active Stage			
Modules Required	Awake Time (ms)	Times (Number/Hour)	Current (mA)	Current per Hour (mA)	Current Per Year (mA)	Battery Use
Xbee	100	10	33	0.0092	80.30	51 %
ATMEGA328P	65	30	1.5	0.0016	14.23	9%
			Measurement Stage			
ADXL345	1.4	60	0.023	0.00001	0.005	0.5%
DHT11	6000	2	1	0.0033	29.20	15%
RG200	135.75	1	200	0.0075	65.70	25%
Rainfall Sensor	100	1	15	0.004	3.65	2%
FC-28	100	5	15	0.0021	18.25	9%
			Transmission Stage			
LoRa 12X78	162.2	5	120	0.0270	236.52	51%
LoRa 12x78	162.2	5	10.8	0.0024	21.29	5%
ATMEGA328P	65	30	1.5	0.0016	14.23	9%
ESP8266	2	30	170	0.0028	24.82	11%

wake-up time, i.e. 6000ms at 25°C. Moreover, it consumes a maximum average of 1mA current with standby consumption is 150μA. The measurement range of DHT11 is 20-90% RH with accuracy ±5%RH, 0-50°C with an accuracy of ±2°C. As temperature and humidity data does not frequently change so only two reading in an hour is more than sufficient. However, it consumed more current against the accelerometer, i.e. 29.20mA, with 15% consumption of battery level. RG200 rain gauge sensor used to measure real-time rainfall with 6'' orifice, mounting brackets, and conductor length of 40 ft. The average switch and settling time is 135.75ms at 30VDC/0.2A. The dimension of the rain gauge is 15 × 38 cm with an operating temperature of 0°C to 51°C. It has an accuracy of 3% up to 4''/hr with a resolution of 0.01 inches. For one reading per hour, it consumes 65.70mA of current and drains 25% battery. A rainfall sensor is also used to measure water level filtration in a different location as rain gauge RS200 is supposed to be deployed as one unit (due to high current consumption) centrally in the monitoring area. Rainfall sensors have digital output as well as analog output also with

a 5V input power supply. It has an LM393 voltage regulator, and current consumption is 15mA while reading and registering values. Moreover, the system comes with a small PCB size of 3.2cm × 1.4cm to deploy the sensor. Its start-up time is 100ms and with 15mA current for one reading in an hour consumes 3.65mA current per year with battery consumption of only 2%. In the measurement stage FC-28 sensor is used to measure soil moisture five times per hour. It consumes 15mA current while reading and registering soil moisture value.
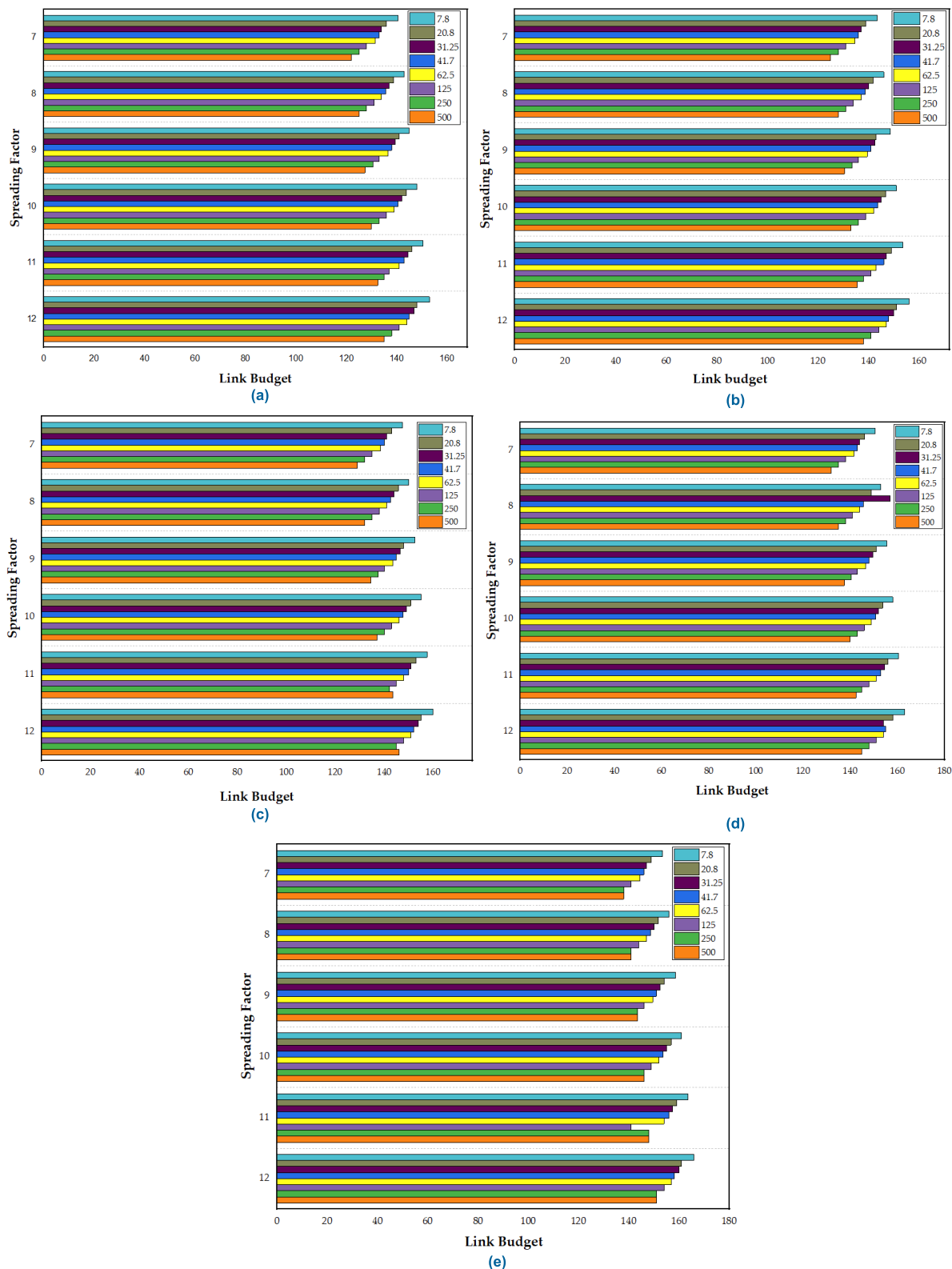
TABLE 9. Comparison table.

Research	Computing Unit	Communication Link	Sensor Node (Customized)	Gateway Node (Customized)	LoRa Metrics	Cloud Infrastructure	Battery Analysis
[38]	Bluefox v2.7	SIGFOX	No	No	No	Yes	Yes
[39]	Waspmote	GSM/GPRS	No	No	No	Yes	No
[40]	Arduino	Zigbee	No	No	No	Yes	No
[41]	IoT Gateway	Zigbee/LoRa	No	No	Yes	Yes	No
[42]	Arduino MKR WAN 1310	Murata CMWX1ZZABZ	No	No	No	Yes	No
Proposed	ATMEGA328P	Zigbee/SX1278 LoRa/ESP8266	Yes	Yes	Yes	Yes	Yes

FIGURE 12. Link budget analysis at (a) 4 dBm (b) 7 dBm (c) 11 dBm (d) 14 dBm (e) 17 dBm.

The requirement of current per hour is 0.021mA, and for the year, it required 18.25mA. It drains 9% of the total battery for five readings per hour.

VII. RESULTS
This section shows the data received on the cloud server of the sensor node and gateway in a real-time case. Testing of LoRa

coverage was performed with a distance of 500m between the gateway and sensor node. Sensors nodes connected with gateway LoRa module at 433MHz to receive data. We placed four accelerometers in different locations, rainfall sensor, soil moisture sensor, temperature, and humidity sensor. The coordinator node successfully placed data on the gateway. Further, the gateway receiving the data and with the help of ESP8266 Wi-Fi module data placed on a cloud server. Figure 13 (a) shows the implementation of the application using MIT app inventor. This platform use coding pattern as block-based. According to the feature, blocks are divided and the outcome shows in Figure 13 (b). The data of rainfall sensor, soil moisture, latitude, and longitude can be seen in the designed application with a level of the warning message. Moreover, according to the received value on the cloud real-time risk alarm will also get display on the application. Application provided emergency tab to use in a real-time environment and as well as help tab to get the working behavior of the app. Figure 13 (b) shows the acceleration impact in different accelerometers placed on the sloped surface. Values are recorded for one day period and on average 3rd accelerometer got a higher impact of changes. Figure 13 (c, d, e, f) illustrates the G-force value of the accelerometer and further store on the cloud server. Moreover, the customized board design is compact for designed for real-time test cases. The device integrates with LoRa module as well as the ESP8266 Wi-Fi module provides adequate results and makes it a low-cost and low-power gateway module. The integration of LCD data can be visualized in the gateway node also. However, the same gateway node data logs on the cloud server through the internet with a time stamp.

Table 9 illustrates the comparison of our proposed work with different studies found in IoT and LoRa based Landslide monitoring systems. The comparison has been done in certain areas like computing units, communication link between transmitter and receiver, customized nodes, cloud access, different LoRa metrics evaluation, and battery analysis in different stages. The proposed study focused on low-cost and energy-efficient customized boards and testing of different useful metrics while the deployment of the system. Distinct parameters like ToA, link budget, sensitivity, data rate, Fresnel zone, and battery life of nodes are evaluated in different bandwidths. The metrics evaluation of LoRa is missing in most of the research in the application of landslide monitoring which plays an important role while deployment in resource less landslide-prone areas. We found significant achievements to record data from customized sensor nodes to the coordinator and the gateway to the cloud server with real-time implementations. In our study we found to decrease the spreading factor from SF12 to 7, increase the data rates, whereas SF 7 provides optimal output to transmit a large amount of data. The sensitivity power is lowest for SF12 at 500KHz. Moreover, Fresnel zone clearance decreases while increasing the distance.
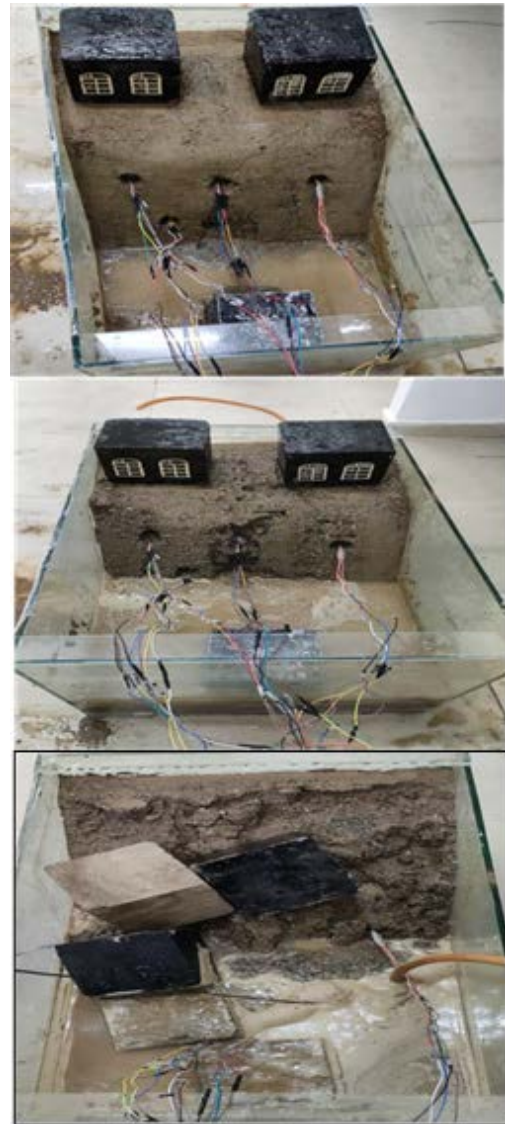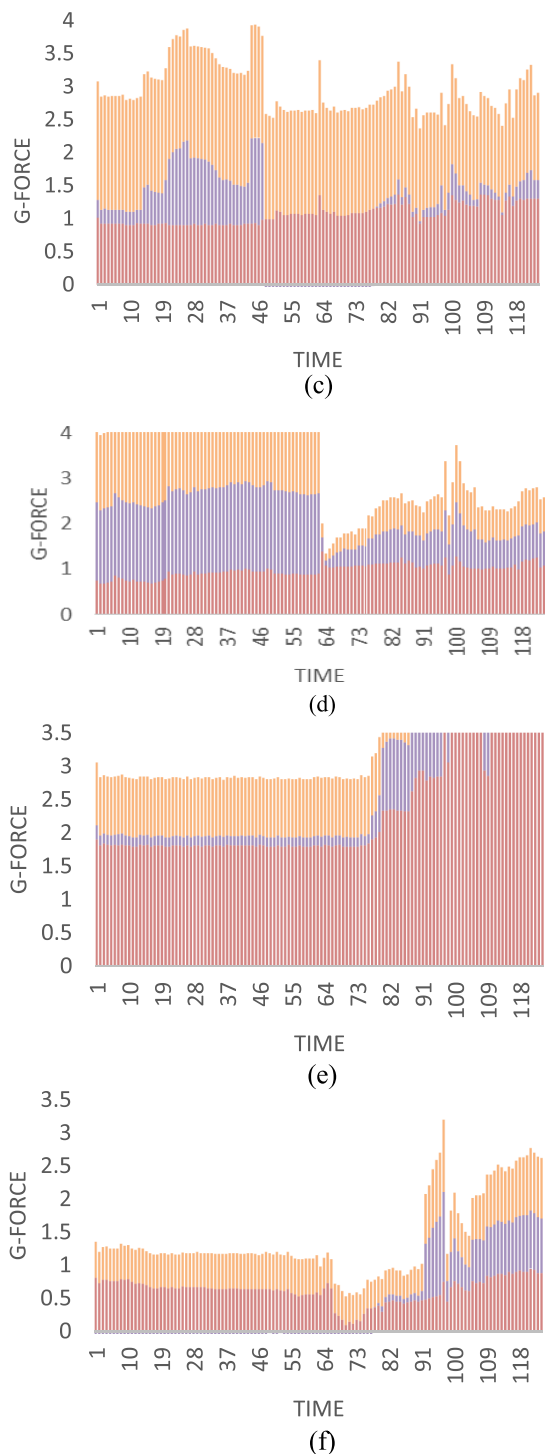

(a)
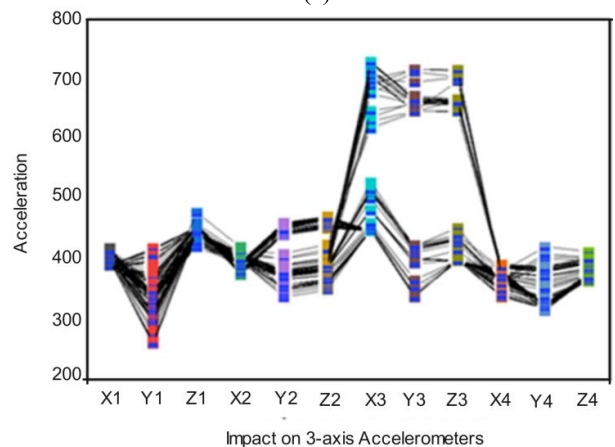
(b)

FIGURE 13. (a) Lab Test bed (b) Accelerators value (c) G-force(g) value at Node1 (d) G-force(g) value at Node2 (e) G-force(g) value at Node3 (f) G-force(g) value at Node4.

FIGURE 13. *(Continued.)* (a) Lab Test bed (b) Accelerators value (c) G-force(g) value at Node1 (d) G-force(g) value at Node2 (e) G-force(g) value at Node3 (f) G-force(g) value at Node4.

VIII. CONCLUSION

In reliable transfer between sensor nodes and a server in IoT, the wireless communication protocol plays a significant role. LoRa is one of the prominent and emerging wireless connections that comply with IoT's minimum energy consumption and long-range communication standards. In this study, we have designed a customized board and tested different metrics of LoRa for the deployment of the system in the Landslide monitoring application. Real-time data gathered from sensors node, further transmitted to coordinator node and finally placed data on IoT server using gateway consist of SX1278 LoRa and ESP8266 Wi-Fi module. We found Spreading factor SF7, ToA is lowest 42.3ms at 500KHz which is optimal to use for this application. Whereas to decrease in the frequency at 125KHz, ToA increase to 169.22ms. We observe sensitivity at 500KHz for SF 7 is highest i.e. −118 and sensitivity at 7.8KHz for SF12 is lowest i.e. −149. We have tested the degradation level of signal with respect to obstacle height in different distance scenarios i.e from 1Km to 10Km. The result illustrates the clearance of the Fresnel area decreases as the distance increases. Battery lifetime is measured in several phases with the minimum quantity of data per hour from the custom sensor node. Moreover, if the frequency of data increased to more numbers per hour battery life for application will be short. The real-time experiment was performed in all the custom nodes and data received on cloud server periodicity. Moreover, the application shows the real-time sensor node data with a deployment map. In the future work prospective customized coordinator node can be enabled with fog computing so end node provides response or warning in real-time situations.

REFERENCES

[1] F. K. Rengers, L. A. McGuire, N. S. Oakley, J. W. Kean, D. M. Staley, and H. Tang, "Landslides after wildfire: Initiation, magnitude, and mobility," *Landslides*, vol. 17, no. 11, pp. 2631–2641, Nov. 2020.

[2] E. G. Franco, "The global risks report 2020," World Econ. Forum, Geneva, Switzerland, Tech. Rep. 15, 2020.

[3] E. Aristizábal and O. Sánchez, "Spatial and temporal patterns and the socioeconomic impacts of landslides in the tropical and mountainous Colombian Andes," *Disasters*, vol. 44, no. 3, pp. 596–618, Jul. 2020.

[4] G. L. R. Peña, L. A. B. Parrales, C. A. G. Rodríguez, and J. H. S. Ramírez, *Las Amenazas por Movimientos en Masa de Colombia: Una Visión a Escala 1:100,000*, 1st ed. Bogotá, Colombia: Servicio Geológico Colombiano, 2017.

[5] D. Zorbas, K. Abdelfadeel, P. Kotzanikolaou, and D. Pesch, "TS-LoRa: Time-slotted LoRaWAN for the industrial Internet of Things," *Comput. Commun.*, vol. 153, pp. 1–10, Mar. 2020.

[6] D. F. Carvalho, P. Ferrari, E. Sisinni, A. Depari, S. Rinaldi, M. Pasetti, and D. Silva, "A test methodology for evaluating architectural delays of LoRaWAN implementations," *Pervasive Mobile Comput.*, vol. 56, pp. 1–17, May 2019.

[7] K. Mekkia, E. Bajica, F. Chaxela, and F. Meyer, "A comparative study of LPWAN technologies for large-scale IoT deployment," *ICT Exp.*, vol. 5, no. 1, pp. 1–7, 2019.

[8] M. Eldefrawy, I. Butun, N. Pereira, and M. Gidlund, "Formal security analysis of LoRaWAN," *Comput. Netw.*, vol. 148, pp. 328–339, Jan. 2019.

[9] Semtech Corporation. (2013). *SX1272/3/6/7/8 LoRa Modem Design Guide, AN1200.13*. [Online]. Available: https://www.rsonline.com/

[10] J. M. Marais, R. Malekian, and A. M. Abu-Mahfouz, "LoRa and LoRaWAN testbeds: A review," in *Proc. IEEE AFRICON*, Sep. 2017, pp.1496–1501.

[11] R. S. Sinha, Y. Wei, and S.-H. Hwang, "A survey on LPWA technology: LoRa and NB-IoT," *ICT Exp.*, vol. 3, no. 1, pp. 14–21, Mar. 2017.

[12] L. Casals, B. Mir, R. Vidal, and C. Gomez, "Modeling the energy performance of LoRaWAN," *Sensors*, vol. 17, no. 10, p. 2364, Oct. 2017.

[13] É. Morin, M. Maman, R. Guizzetti, and A. Duda, "Comparison of the device lifetime in wireless networks for the Internet of Things," *IEEE Access*, vol. 5, pp. 7097–7114, 2017.

[14] H. T. Reda, P. T. Daely, J. Kharel, and S. Y. Shin, "On the application of IoT: Meteorological information display system based on LoRa wireless communication," *IETE Tech. Rev.*, vol. 35, no. 3, pp. 256–265, May 2018.

[15] T. Bouguera, J.-F. Diouris, J.-J. Chaillout, R. Jaouadi, and G. Andrieux, "Energy consumption model for sensor nodes based on LoRa and LoRaWAN," *Sensors*, vol. 18, no. 7, p. 2104, Jun. 2018.

[16] V. Sharma, I. You, G. Pau, M. Collotta, J. Lim, and J. Kim, "LoRaWAN-based energy-efficient surveillance by drones for intelligent transportation systems," *Energies*, vol. 11, no. 3, p. 573, Mar. 2018.

[17] T. Popović, N. Latinović, A. Pešić, Ž. Zečević, B. Krstajić, and S. Djukanović, "Architecting an IoT-enabled platform for precision agriculture and ecological monitoring: A case study," *Comput. Electron. Agricult.*, vol. 140, pp. 255–265, Aug. 2017.

[18] A. Botta, W. de Donato, V. Persico, and A. Pescapé, "Integration of cloud computing and Internet of Things: A survey," *Future Gener. Comput. Syst.*, vol. 56, pp. 684–700, Mar. 2016.

[19] T. Ameloot, P. Van Torre, and H. Rogier, "A compact low-power LoRa IoT sensor node with extended dynamic range for channel measurements," *Sensors*, vol. 18, no. 7, p. 2137, Jul. 2018.

[20] D. K. Yadav, P. Mishra, S. Jayanthu, and S. K. Das, "Fog-IoT-based slope monitoring (FIoTSM) system with LoRa communication in open-cast mine," *IEEE Trans. Instrum. Meas.*, vol. 70, pp. 1–11, 2021.

[21] E. Goldoni, L. Prando, A. Vizziello, P. Savazzi, and P. Gamba, "Experimental data set analysis of RSSI-based indoor and outdoor localization in LoRa networks," *Internet Technol. Lett.*, vol. 2, no. 1, pp. e75–e80, Jan. 2019.

[22] J. Li, C. K. Li, K. Li, and Y. Liu, "Design of landslide monitoring and early warning system based on Internet of Things," *Appl. Mech. Mater.*, vols. 511–512, pp. 197–201, Feb. 2014, doi: 10.4028/www.scientific.net/AMM.511-512.197.

[23] M. Krkac, D. Špoljarić, S. Bernat, and S. M. Arbanas, "Method for prediction of landslide movements based on random forests," *Landslides*, vol. 14, no. 3, pp. 947–960, 2017, doi: 10.1007/s10346-016-0761-z.

[24] R. Franceschini, A. Rosi, F. Catani, and N. Casagli, "Exploring a landslide inventory created by automated web data mining: The case of Italy," *Landslides*, vol. 19, no. 4, pp. 841–853, Apr. 2022.

[25] B. Buurman, J. Kamruzzaman, G. Karmakar, and S. Islam, "Low-power wide-area networks: Design goals, architecture, suitability to use cases and research challenges," *IEEE Access*, vol. 8, pp. 17179–17220, 2020.

[26] LoRa Alliance. (2016). *LoRa-Alliance Technology*. Accessed: Nov. 2019. [Online]. Available: https://www.lora-alliance.org/technology

[27] Semtech Corporation. (2015). *LoRa Modulation Basics AN1200.22*. Accessed: Nov. 2019. [Online]. Available: https://www.semtech.com/uploads/documents/

[28] C. Goursaud and J. M. Gorce, "Dedicated networks for IoT: PHY/MAC state of the art and challenges," *EAI Endorsed Trans. Internet Things*, vol. 1, no. 1, Oct. 2015, Art. no. 150597.

[29] M. Bor, J. Vidler, and U. Roedig, "LoRa for the Internet of Things," in *Proc. Int. Conf. Embedded Wireless Syst. Netw. (EWSN)*, 2016, pp. 361–366.

[30] A. M. Yousuf, E. M. Rochester, and M. Ghaderi, "A low-cost LoRaWAN testbed for IoT: Implementation and measurements," in *Proc. IEEE 4th World Forum Internet Things (WF-IoT)*, Feb. 2018, pp. 361–366, doi: 10.1109/WF-IoT.2018.8355180.

[31] Semtech Corporation. (2016). *SX1276/77/78/79-137 MHz to 1020 MHz Low Power Long Range Transceiver*. [Online]. Available: https://www.scribd.com/document/399165229/SX1276-1278

[32] Semtech. *SX1272/73 Low Power Long Range Transceiver*. Accessed: Dec. 2018. [Online]. Available: https://www.semtech.com/uploads/documents/sx1272.pdf

[33] E. Sallum, N. Pereira, M. Alves, and M. Santos, "Improving quality-of-service in LoRa low-power wide-area networks through optimized radio resource management," *J. Sens. Actuator Netw.*, vol. 9, no. 1, p. 10, Feb. 2020.

[34] *LoRaTool*. Accessed: Apr. 1, 2021. [Online]. Available: https://www.loratools.nl

[35] T. Sherwin, M. Easte, A. Chen, K. Wang, and W. Dai, "A single RF emitter-based indoor navigation method for autonomous service robots," *Sensors*, vol. 18, no. 2, p. 585, Feb. 2018.

[36] D. D. Coleman and D. A. Westcott, *CWNA Certified Wireless Network Administrator Official Study Guide: Exam PW0-104*. New York, NY, USA: Wiley, 2009.

[37] S. M. Karunarathne, M. Dray, L. Popov, M. Butler, C. Pennington, and C. M. Angelopoulos, "A technological framework for data-driven IoT systems: Application on landslide monitoring," *Comput. Commun.*, vol. 154, pp. 298–312, Mar. 2020.

[38] Q. A. Gian, D.-T. Tran, D. C. Nguyen, V. H. Nhu, and D. T. Bui, "Design and implementation of site-specific rainfall-induced landslide early warning and monitoring system: A case study at Nam Dan landslide (Vietnam)," *Geomatics, Natural Hazards Risk*, vol. 8, no. 2, pp. 1978–1996, Dec. 2017.

[39] R. Dhanagopal and B. Muthukumar, "A model for low power, high speed and energy efficient early landslide detection system using IoT," *Wireless Pers. Commun.*, vol. 117, no. 4, pp. 2713–2728, Apr. 2021.

[40] S. Kumar, P. V. Rangan, and M. V. Ramesh, "Design and validation of wireless communication architecture for long term monitoring of landslides," in *Proc. Workshop World Landslide Forum*. Cham, Switzerland: Springer, 2017, pp. 51–60.

[41] M. Gamperl, J. Singer, and K. Thuro, "Internet of Things geosensor network for cost-effective landslide early warning systems," *Sensors*, vol. 21, no. 8, p. 2609, Apr. 2021.

SWAPNIL BAGWARI received the M.Tech. degree in embedded systems from Punjab Engineering College, Chandigarh, India, in 2009. He is currently pursuing the Ph.D. degree in electronics and communication engineering with Lovely Professional University. He is associated with Lovely Professional University as an Assistant Professor with more than ten years of experience in academics. He has one patent granted and 35 patents published in his account. He has published more than ten research papers in refereed journals and conferences. He has organized several summer internships and expert lectures for students in the field of the IoT and embedded systems.

AJAY ROY received the Engineering degree from the West Bengal University of Technology and the Ph.D. degree in electronics from Dr. B. R. Ambedkar National Institute of Technology, Jalandhar, India. He is currently associated with Lovely Professional University as an Associate Professor with more than 12 years of experience in academics. His areas of expertise include embedded systems, robotics, wireless sensor networks, the Internet of Things, and machine learning. He has published more than 40 research papers in referred journals/conferences. He has been honored as a keynote speaker and the session chair to international/national conferences, faculty development programs, workshops, and webinars. He has guided two Ph.D. scholars and currently guiding nine Ph.D. scholars.

ANITA GEHLOT is associated with Lovely Professional University as an Associate Professor with more than ten years of experience in academics. She has four patents granted and 20000 published in her account. She has published more than 50 research papers in refereed journals and conferences. She has organized several workshops, summer internships, and expert lectures for students. She has been awarded a "Certificate of Appreciation" from the University of Petroleum and Energy Studies for exemplary work. She has published ten books in the area of embedded systems and the Internet of Things with reputed publishers like CRC/Taylor & Francis, Narosa, GBS, IRP, NIPA, and RI publication. She is an Editor of a Special Issue published by the AISC book series with the title "*Intelligent Communication, Control and Devices*" (Springer, 2018).

RAJESH SINGH received the B.E. and M.Tech. degrees (Hons.). He is currently associated with Lovely Professional University as a Professor with more than 15 years of experience in academics. His areas of expertise include embedded systems, robotics, wireless sensor networks, and the Internet of Things. He has organized and conducted several workshops, summer internships, and expert lectures for students as well as faculty. He has four patents published and more than 100 patents published in his account. He has published over 100 research papers in refereed journals/conferences. He has published ten books in the area of embedded systems and the Internet of Things with reputed publishers like CRC/Taylor & Francis, Narosa, GBS, IRP, NIPA, and RI publication. Under his mentorship, students have participated in national/international competitions, including the Texas competition in Delhi and the Laureate Award of Excellence in robotics engineering in Spain. Twice in the last four years, he has been awarded a "Certificate of Appreciation" and the "Best Researcher Award-2017" from the University of Petroleum and Energy Studies for exemplary work. He received a "Certificate of Appreciation" for mentoring the projects submitted to the Texas Instruments Innovation challenge India design contest, from Texas Instruments, in 2015. He is an Editor of a Special Issue published by the AISC book series with the title "*Intelligent Communication, Control and Devices*" (Springer, 2017 and 2018).

NEERAJ PRIYADARSHI (Senior Member, IEEE) received the M.Tech. degree in power electronics and drives from the Vellore Institute of Technology (VIT), Vellore, India, in 2010, and the Ph.D. degree from the Government College of Technology and Engineering, Udaipur, Rajasthan, India. He is currently associated with the Department of Energy Technology, Aalborg University, Esbjerg, Denmark, where he has held postdoctoral position in bioenergy and green engineering with the Department of Energy Technology. In previous postings, he was with BITT Ranchi, MIT Purnea, JK University, Geetanjali Institute, Global Institute, and SS Group, Rajasthan, India. His current research interests include power electronics, control systems, power quality, and solar power generation. He has published over 60 papers in journals and conferences of high repute like IEEE SYSTEMS JOURNAL, *IET Electric Power Applications*, *IET Power Electronics*, IEEE ACCESS, *Electric Power Components and Systems*, *International Transactions on Electrical Energy Systems* (Wiley), *Energies* (MDPI), and *International Journal of Renewable Energy Research*, and granted ten international patents. He successfully organized two international workshops and one national workshop in different organization. He is also invited as a guest speaker in many international/national conferences. He is a Reviewer of IEEE TRANSACTIONS ON INDUSTRIAL INFORMATICS, IEEE TRANSACTIONS ON INDUSTRY APPLICATIONS, IEEE SYSTEMS JOURNAL, *Journal of Cleaner Production* (Elsevier), *International Journal of Electrical Power & Energy Systems*, *IET Power Electronics*, *Energy for Sustainable Development* (Elsevier), *Energy Reports* (Elsevier), *Sustainable Energy Technologies and Assessments* (Elsevier), *International Journal of Energy Research* (Wiley), *Electronics Letters* (IET), *Electric Power Components and Systems* (Taylor & Francis), IEEE ACCESS, *IET Renewable Power Generation*, *International Journal of Modelling and Simulation*, *International Journal of Renewable Energy Research*, *International Journal of Power Electronics and Drive Systems*, and reputed Elsevier SCI indexed journals. Under his guidance 25 DST, Government of Rajasthan projects have been sanctioned for financial support. He is working as the Chief Editor of four edited books of renowned publisher [*Intelligent Renewable Energy Systems: Integrating Artificial Intelligence Techniques and Optimization Algorithms* (Wiley) and *Advances in Power Systems and Energy Management* (Springer and De Gruyter Publisher, Germany)].

BASEEM KHAN (Senior Member, IEEE) received the B.Eng. degree in electrical engineering from Rajiv Gandhi Technological University, Bhopal, India, in 2008, and the M.Tech. and D.Phil. degrees in electrical engineering from the Maulana Azad National Institute of Technology, Bhopal, India, in 2010 and 2014, respectively. He is currently working as a Faculty Member at Hawassa University, Ethiopia. His research interests include power system restructuring, power system planning, smart grid technologies, metaheuristic optimization techniques, reliability analysis of renewable energy systems, power quality analysis, and renewable energy integration.

• • •